Available online at www.sciencedirect.com
SCIENCE DIRECT®
Journal of Catalysis 236 (2005) 366–378
JOURNAL OF CATALYSIS
www.elsevier.com/locate/jcat

Ethylene epoxidation over silver and copper–silver bimetallic catalysts: I. Kinetics and selectivity

Jerome T. Jankowiak, Mark A. Barteau *

Center for Catalytic Science and Technology (CCST), Department of Chemical Engineering, University of Delaware, Newark, DE 19716, USA

Received 1 July 2005; revised 8 October 2005; accepted 11 October 2005

Available online 11 November 2005

Abstract

Copper–silver bimetallic catalysts offer improved selectivities compared with silver alone in the direct epoxidation of ethylene. This bimetallic combination was previously identified by density functional theory calculations, and its performance advantage was verified in preliminary catalytic reactor experiments. We report here a more detailed investigation of the performance of monolith-supported silver and Cu–Ag bimetallic catalysts at different feed compositions and reaction temperatures. From these studies, information about activation energies and reaction orders for ethylene epoxidation was obtained. The superior performance of the Cu–Ag bimetallic catalysts prepared by sequential impregnation was demonstrated over a wide range of feed compositions.

Keywords: Ethylene epoxidation; Silver catalysts; Bimetallic catalyst; Oxametallacycle; Monolith catalysts

1. Introduction

The silver-catalyzed epoxidation of ethylene with oxygen is one of the most important and successful examples of heterogeneous catalysis to date. Ethylene oxide (EO) has long been one of the highest volume chemicals produced by the chemical industry, accounting for approximately 40–50% of the total value of organic chemicals produced by heterogeneous oxidation [1,2]. In 1998, >8 billion pounds of ethylene oxide were produced worldwide [3]. The process uses a silver catalyst supported on α-Al_2O_3, promoted by alkalis and halides. The principal nonselective product is carbon dioxide. The formation of carbon dioxide is highly exothermic, and the process is run at low conversions (<15%) to achieve high selectivities and to control the heat released by combustion. More selective catalysts can improve operability by reducing the heat generated by the process.

Previous work from this laboratory has provided new insights into the mechanism of ethylene epoxidation. A combination of surface science studies and quantum chemical calculations was used to isolate and identify a surface oxametallacycle as the common intermediate participating in both the selective and nonselective pathways [4]. This intermediate can react to form EO or acetaldehyde, with both processes having similar activation energies. It has been shown previously that acetaldehyde is rapidly oxidized on silver to form carbon dioxide [5,6], and thus it has been postulated that acetaldehyde is the gateway for the production of CO_2. The transition state structures and energy barriers for the formation of EO and acetaldehyde from the oxametallacycle intermediate have been obtained using quantum chemical calculations [4].

The development of a mechanistic understanding for the formation of EO and carbon dioxide led to the design of a more selective catalyst from first principles [7]. Quantum chemical calculations suggested that a Cu–Ag bimetallic catalyst should be more selective than pure silver toward EO. This prediction was verified by conducting a series of steady-state reactor experiments exploring the performance of monolith-supported silver and Cu–Ag bimetallic catalysts for a feed stream containing 10% oxygen and 10% ethylene at 1.34 atm (5 psig). The Cu–Ag bimetallic catalysts were approximately 1.5 times more selective than the pure silver catalysts at optimal copper loadings.

* Corresponding author. Fax: +1 302 831 8201.
E-mail address: barteau@che.udel.edu (M.A. Barteau).

0021-9517/$ – see front matter
doi:10.1016/j.jcat.2005.10.018

Besides being more selective, the Cu–Ag bimetallic catalysts were also more active.

The purpose of the present work was to explore the performance of Cu–Ag bimetallic catalysts over a wider range of feed compositions and reaction temperatures. From these experiments, the performance of the Cu–Ag catalysts relative to that of pure silver with respect to EO selectivity was evaluated, and kinetics information about the process over these catalysts was obtained.

To put these results in context, it is useful to consider recent models for the kinetics and mechanism of this process. The essential features of the mechanism of ethylene epoxidation can be represented by a minimum of four elementary steps [8]:

$$O_2(g) + 2* \leftrightarrows 2O(a), \quad (1)$$

$$C_2H_4(g) + * \leftrightarrows C_2H_4(a), \quad (2)$$

$$C_2H_4(a) + O(a) \leftrightarrows CH_2CH_2O(a) + *, \quad (3)$$

$$CH_2CH_2O(a) \leftrightarrows C_2H_4O(g) + *, \quad (4)$$

where (g) represents gas-phase species, (a) represents adsorbed species, and * represents unoccupied surface sites. The mechanism involves two adsorption steps, one of which involves the dissociative adsorption of oxygen, one surface reaction step in which adsorbed ethylene and oxygen react to form the proposed oxametallacycle intermediate, labeled as $CH_2CH_2O(a)$, and one reaction/desorption step in which the intermediate reacts to release gas-phase EO.

Linic et al. [8] and Stegelmann et al. [9,10] have developed microkinetic models for this process. The process actually has two kinetically relevant steps: dissociative adsorption of oxygen and reaction of adsorbed ethylene with adsorbed oxygen atoms. The rate-determining step of the process is therefore governed by the reaction conditions used. The identification of more than one kinetically relevant step has been supported by catalytic studies. Table 1 gives the results of some studies that investigated the kinetics of ethylene epoxidation [11–23]. Listed are the measured apparent activation energies and reaction orders for the formation of EO and CO_2 for studies conducted over a range of reaction conditions and fitted with power-law kinetics.

Table 1
Activation energies (E_a, kcal/mol) and reaction orders (n) for epoxidation (1) and total oxidation (2) of ethylene over silver catalysts

Epoxidation			Total oxidation			Reference
E_{a_1}	$n_{C_2H_4}$	n_{O_2}	E_{a_2}	$n_{C_2H_4}$	n_{O_2}	
16	1	0	16	1	0	[11]
12	0	1	15	0	1	[12]
19	0.3	0.7	–	–	–	[13]
15	–	–	20	–	–	[14]
20	0	1	33	–	–	[15]
9	0.5	0	8	0.5	0	[16]
–	0	1	–	0	1	[17]
–	1	1.5	–	1	2	[18]
–	1	−0.3–1.5	–	1	−0.3–1.5	[19]
–	−0.03	0.91	–	−0.2	1.1	[20]
$E_{a_1} = E_{a_2}$	1	0.5	$E_{a_1} = E_{a_2}$	1	0.5	[21]
25	1	0.5	24	1	0.5	[22]
18	0.7	1	15	0.7	1	[23]

The similarity of the calculated activation barriers for dissociative oxygen adsorption and surface reaction makes it difficult to identify the rate-determining step of the process on the basis of these barriers alone [8]. Nonetheless, determining reaction orders for oxygen and ethylene can help identify the rate-determining step of the process. For conditions in which the dissociative adsorption of oxygen is rate-determining, the rate of reaction would be expected to be enhanced by an increase in oxygen pressure and to display little or no dependence on ethylene pressure. In this case, the reaction order in oxygen would be positive, whereas the reaction order in ethylene would be approximately zero. For conditions in which the surface reaction is rate-determining, the rate of reaction should be influenced by changes in both oxygen pressure and ethylene pressure, yielding positive reaction orders for both components.

As shown in Table 1, the reaction orders reported for the formation of EO from oxygen and ethylene vary significantly. Reaction orders of 0–1.5 for oxygen and −0.03–1 for ethylene have been reported. These variations can likely be attributed to variations in reaction conditions used to study the kinetics, and highlight the presence of multiple kinetically relevant steps in the process. Apparent activation energies for EO formation reportedly range from 9 to 22 kcal/mol, with an average of approximately 16 kcal/mol. For CO_2 formation, the measured reaction orders of oxygen and ethylene have been reported in ranges of −0.3–1.5 and −0.2–1, respectively. Measured apparent activation energies for CO_2 formation have been reported to be either comparable to or slightly higher than those for EO formation, with reported values in the range of 8–33 kcal/mol.

As we show below, our results for monolith-supported silver and copper–silver bimetallic catalysts at 1.34 atm show activation energies and reaction orders near the median values of the ranges reported in the literature. Under these conditions, the bimetallic catalysts exhibit higher activities and epoxidation selectivities over a wide range of ethylene/oxygen ratios.

2. Experimental

The methods used for catalyst preparation and reactor operation have been described previously [7]. Catalyst supports were ceramic foam monoliths (99.5% α-Al_2O_3) from Vesuvius Hi-Tech Ceramics. The monoliths used for this study had 45 pores per linear inch (ppi), corresponding to a porosity of approximately 80%, and measured 18 mm diameter ×10 mm long. The surface area of these monoliths was measured by BET analysis as approximately 0.3 m^2/g. Surface areas of the finished, metal-loaded monoliths containing 11–13 wt% metal were within 10% of this value. Because of some batch-to-batch variability, direct performance comparisons between catalysts with different metals content are made only for catalysts prepared from the same monolith batch.

Before use, all monoliths were cleaned by boiling in distilled water for 1 h, followed by baking in air at 80 °C until dry (typically 2 h). Catalysts were prepared by wet impregnation techniques. Monoliths were contacted with an aqueous solution of silver nitrate ($AgNO_3$) slightly in excess of the amount required for incipient wetness, then dried in air at 80 °C. The

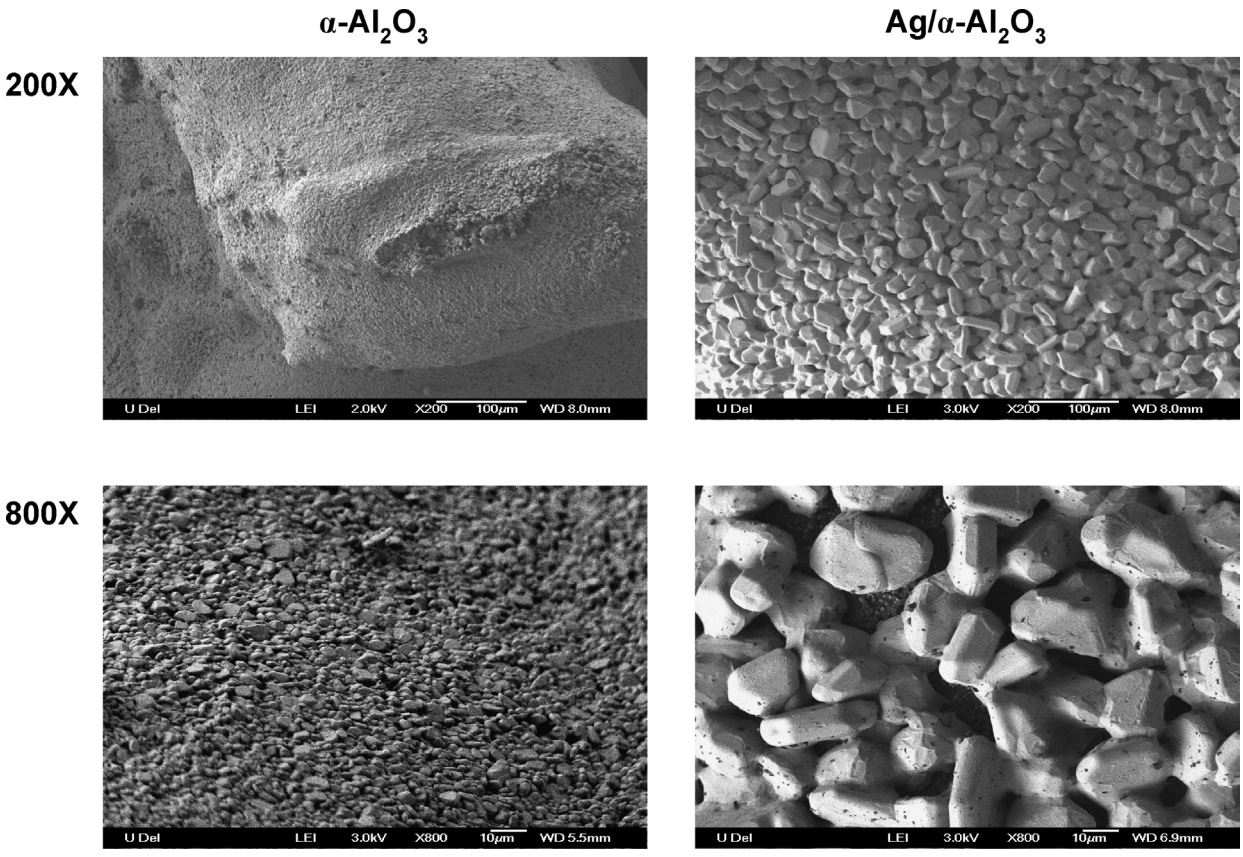

Fig. 1. Scanning electron micrographs of an α-Al_2O_3 monolith before and after silver deposition.

monolith catalyst was then calcined at 400 °C for 12 h in an open-air furnace, and reduced in flowing H_2/He (20% H_2 by volume) at 300 °C for an additional 12 h in situ before the start of the reaction. Catalyst samples contained silver loadings of approximately 11–13 wt% of active catalyst. For the copper-promoted catalysts, copper was added in the form of aqueous cupric nitrate [$Cu(II)(NO_3)_2$] to the reduced silver catalyst via wet impregnation, using a solution with a copper concentration of 1 g/L. After addition of the cupric nitrate, the catalysts were exposed to a flowing stream of H_2/He for 12 h at 300 °C to reduce the cupric nitrate to metallic copper.

We have previously reported XPS results for bimetallic catalysts prepared by this sequential impregnation and reduction process [7]. These results demonstrated that catalysts containing Cu/Ag atom ratios of 0.001–0.01 exhibited surface Cu/Ag ratios of 0.1–0.75. For a catalyst with a Cu/Ag atom ratio of 0.002, which we estimate from XPS to have a surface Cu/Ag ratio of 0.25, the total Cu loading represents a maximum coverage of 0.5 monolayers on a total catalyst area of 0.3 m^2/g. Thus it is clear that Cu is highly dispersed. Although we cannot rule out the possibility that some copper is located on the support rather than on the silver surface, electron microscopy data (shown below) demonstrate that the monolith surface is nearly completely covered by silver at the Ag loadings used. In the absence of any evidence to the contrary, it is reasonable to conclude that the sequential impregnation technique produces significant enrichment of Cu on the silver surface, generating materials that correspond reasonably well to the design basis (25 at% Cu at the Ag surface) for the density functional theory (DFT) calculations that predicted superior performance of Cu–Ag bimetallics [7].

Scanning electron microscopy (SEM) was used to image supported silver and Cu–Ag bimetallic catalysts. Experiments were conducted using a JEOL 7400 scanning electron microscope equipped with a cold field emission source operated at 2–3 kV with a limit of resolution of ∼1.5 nm. The accelerating voltage was kept low to prevent beam damage and potential charging effects. The working distance (objective lens to specimen) was 8 mm. Fig. 1 shows SEM images of the bare α-alumina and supported silver catalysts prepared in this study. The silver crystallites were tablet-shaped and 10–20 μm in size, and they covered the α-alumina surface. When a Cu–Ag bimetallic catalyst was prepared by sequential impregnation of Cu at the levels used here, there was no evidence in the micrographs of the formation of particles or surface features of a different size or shape than those illustrated for the supported silver catalyst. SEM elemental analysis of the silver and Cu–Ag bimetallic surfaces confirmed the presence of silver in these particles. However, the element detection system was not sensitive enough to detect copper at the loadings used (65–650 ppm with respect to total catalyst mass).

A schematic of the reactor apparatus is shown in Fig. 2. The reactor comprised an 18-inch-long quartz tube with an outer diameter of 25.4 mm and an inner diameter of 22 mm, slightly larger than the diameter of the foam monolith catalyst. The circumference of the monolith was wrapped with a layer of quartz

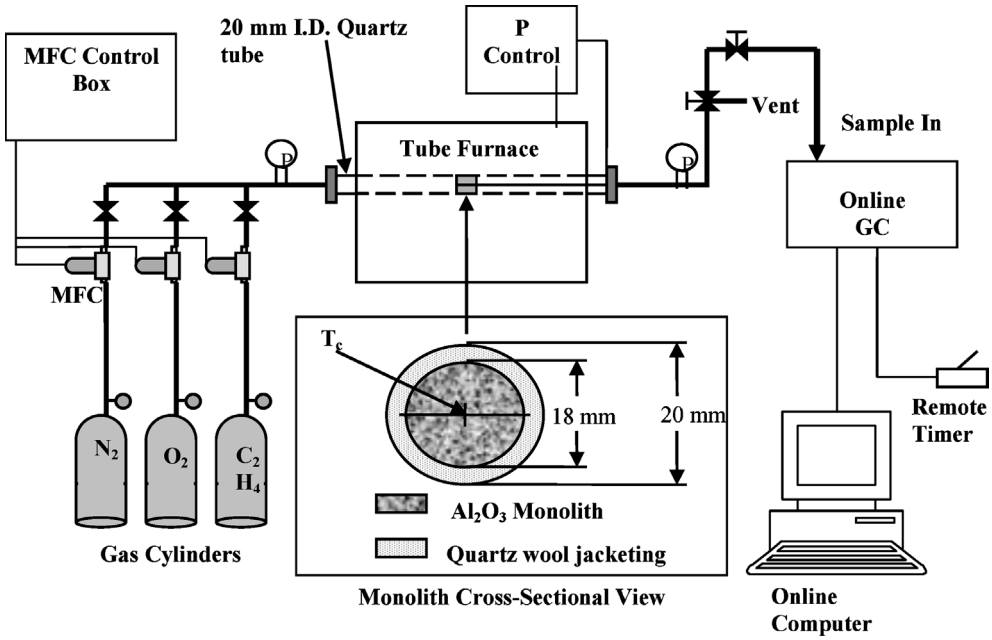

Fig. 2. Reactor schematic.

wool to prevent bypassing of the reactant gas around the catalyst. The monolith was then placed at the center of the quartz tube, which was enclosed in a tube furnace. The reactor tube was connected to the gas handling system by metal compression fittings with Viton o-rings.

Gas flow to the reactor was controlled by electronic mass flow controllers. Reactor pressure was controlled by a needle valve, the outlet of which was vented to the atmosphere, placed just before the inlet of the on-line gas chromatograph. The product gases were fed through heated stainless steel lines to an automated gas chromatograph (Hewlett Packard model 6890) for analysis. The gas chromatograph contained a capillary column (Supelco Plot-Q) for separation of hydrocarbon species, C_2H_4 and EO, which were detected by a flame ionization detector. A second set of columns, consisting of a pair of packed Haysep columns (types N and Q), which separate heavier hydrocarbons (C_{3+}) from lighter hydrocarbons and gases, and a molecular sieve, which separates the atmospheric gases, such as H_2, N_2 and O_2, led to a thermal conductivity detector (TCD). The TCD was used for quantification of CO_2, C_2H_4, N_2, and O_2.

The catalyst temperature was measured using a type K fine-gauge bare-wire thermocouple inserted from the rear of the reactor and placed on the front face of the catalyst. The temperature of the catalyst was controlled with an external proportional controller. The controller maintained the desired set-point temperature to within $\pm 1\,^{\circ}C$.

All experiments were conducted at a reactor pressure of 1.34 atm with a total feed rate of 100 sccm (at STP), giving a contact time on the order of 0.5 s. Industrial ethylene epoxidation processes are carried out both with ethylene-rich conditions (oxygen-based process) and equimolar to slightly oxygen-rich conditions (air-based process). For the oxygen-based process, typical ethylene-to-oxygen ratios of 3:1 to 4:1 are used, whereas the air-based process is typically run at an ethylene-to-oxygen ratio of 1:2. The catalysts discussed here were tested over a wide range of feed conditions ranging from 6:1 ethylene to oxygen to 6:1 oxygen to ethylene, to study the performance of Cu–Ag bimetallic catalysts compared with pure silver catalysts. Two batches of catalysts were studied. Batches are defined as catalysts prepared from the same batch of monoliths and the same lots of silver and copper precursor. The two batches are denoted as batch A and batch B. (Note that these batches do not correspond to the similarly labeled batches described in previous work [7].)

3. Results

All catalysts were lined out for an initial 24-h period of operation under the same feed and temperature conditions. During this period, the feed contained 10 mol% each of oxygen and ethylene, and the reactor temperature was maintained at 540 K. Once a catalyst had been lined out, composition and temperature variation experiments were carried out to probe the kinetics and selectivity of the reaction. After each change of temperature or composition, the reactor was operated at steady state for a minimum of 1 h before the results were recorded. Figs. 3 and 4 illustrate the conversion and selectivity transients for silver and copper–silver bimetallic catalysts during the initial lining-out period, demonstrating that steady state was reached with this procedure.

Figs. 5 and 6 show reaction rate data collected at 540 K for silver and Cu–Ag bimetallic catalysts from batch A for both ethylene-rich and oxygen-rich feed streams. In these experiments the minor feed component was held at 0.13 atm (10 mol%), whereas the major feed component was increased from 0.13 to 0.8 atm (from 10 to 60 mol%), with a balance of nitrogen. The rate of ethylene consumption was not significantly affected by an increase in ethylene feed pressure, but

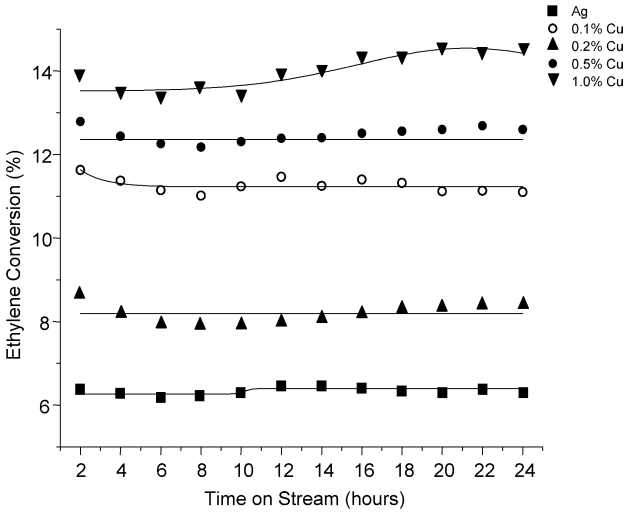

Fig. 3. Measured ethylene conversion as function of time on stream for Ag and Cu–Ag bimetallic catalysts from batch A. The feed stream contained 10% ethylene, 10% oxygen, and 80% nitrogen at a total reactor pressure of 1.34 atm and a temperature of 540 K.

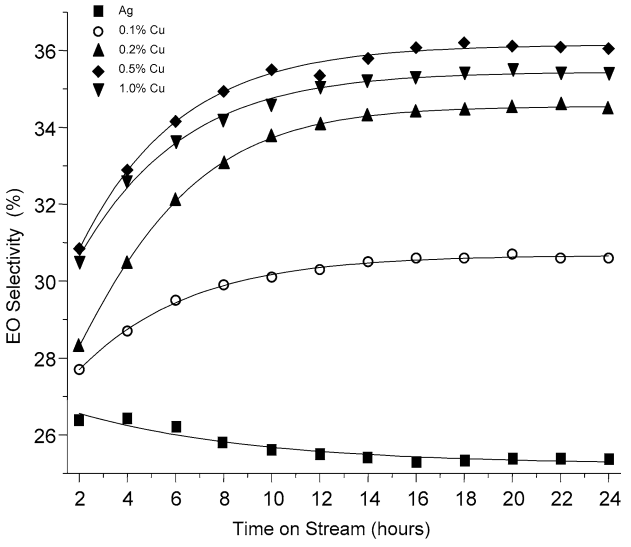

Fig. 4. Measured ethylene oxide selectivity as function of time on stream for Ag and Cu–Ag bimetallic catalysts from batch A. The feed stream contained 10% ethylene, 10% oxygen, and 80% nitrogen at a total reactor pressure of 1.34 atm and a temperature of 540 K.

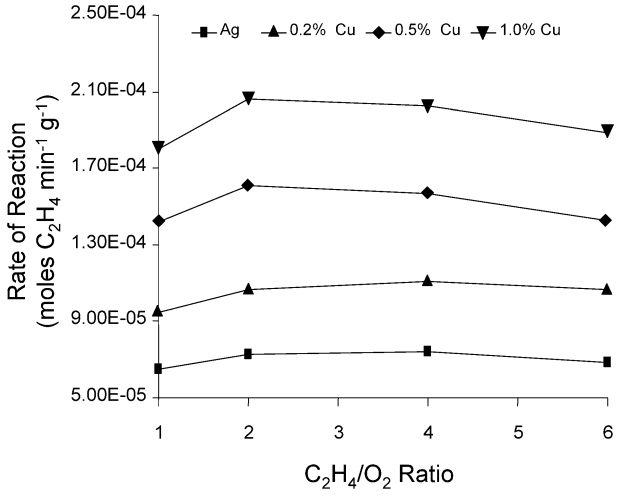

Fig. 5. Measured rates of ethylene reaction at 540 K for silver and Cu–Ag bimetallic catalysts from batch A with ethylene-rich feed streams. The feed stream contained 10% oxygen and 10–60% ethylene.

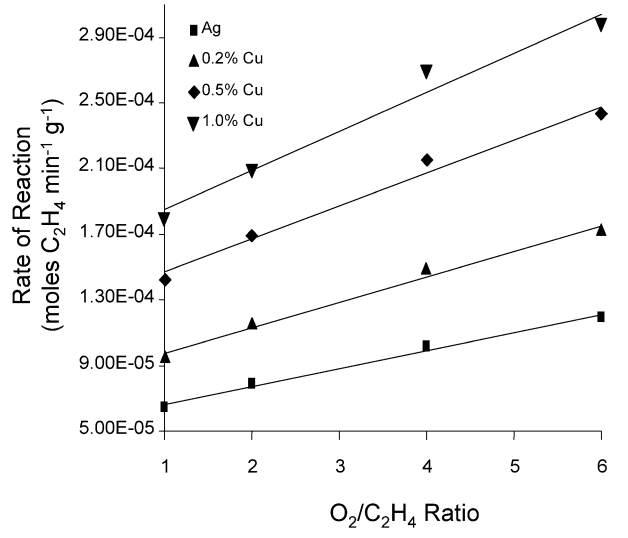

Fig. 6. Measured rates of ethylene reaction at 540 K for silver and Cu–Ag bimetallic catalysts from batch A with oxygen-rich feed streams. The feed stream contained 10% ethylene and 10–60% oxygen.

was measurably affected by an increase in oxygen feed pressure. In agreement with our previous report [7], the Cu–Ag bimetallic catalysts were more active than the pure silver catalyst for all feed conditions used. Similar rate measurements were conducted at 500 and 520 K, in addition to 540 K. From these measurements, apparent activation energies and reaction orders were obtained for the consumption of ethylene and the formation of EO and carbon dioxide over a wide range of feed conditions. These studies are described below.

Activation energy determinations were conducted for silver and Cu–Ag bimetallic catalysts from batches A and B for reactor temperatures of 500–540 K. Summaries of the measured ethylene conversions for catalysts from batches A and B are represented in Tables 2 and 3, respectively, for temperatures of 500 to 540 K and ethylene and oxygen feed compositions ranging from 10 to 60% (from 0.13 to 0.8 atm). It is evident that the inherent activities of the two batches of catalysts are quite different, with catalysts from batch A being significantly more active. This further emphasizes the problem of batch variability discussed previously [7]. Nonetheless, the comparison of silver and Cu–Ag bimetallic catalysts of different base silver activities provided a good measure of the performance enhancements attained with copper modification for different base cases of catalyst performance. It is evident from the data in Tables 2 and 3 that, regardless of the base silver catalyst performance, the activity of the catalyst was significantly enhanced by the addition of copper.

Representative activation energy determinations for a silver catalyst from batch A for ethylene-rich and oxygen-rich feed conditions are shown in Figs. 7 and 8, respectively. It is evident that the activation energy for ethylene consumption was

Table 2
Measured ethylene conversions for silver and Cu–Ag bimetallic catalysts from batch A at 500–540 K and ethylene and oxygen feed concentrations of 10–60%

	Ag	0.2% Cu–Ag	0.5% Cu–Ag	1.0% Cu–Ag
540 K, 10% O_2				
C_2H_4				
10%	6.37	7.73	12.69	14.45
20%	3.57	4.37	7.20	8.27
40%	1.82	2.27	3.51	4.06
60%	1.12	1.45	2.13	2.52
540 K, 10% C_2H_4				
O_2				
10%	6.37	7.73	12.69	14.45
20%	7.73	9.33	15.14	16.70
40%	9.98	12.13	19.19	21.54
60%	11.78	14.06	21.71	23.82
520 K, 10% O_2				
C_2H_4				
10%	4.33	5.62	8.6	9.45
20%	2.29	6.21	4.87	5.46
40%	1.04	7.86	2.24	2.54
60%	0.64	8.92	1.29	1.55
520 K, 10% C_2H_4				
O_2				
10%	4.33	5.62	8.6	9.45
20%	5.01	6.21	9.97	11.43
40%	6.55	7.86	12.47	14.00
60%	7.56	8.92	14.02	15.82
500 K, 10% O_2				
C_2H_4				
10%	2.42	3.10	5.06	5.89
20%	1.24	1.67	2.65	3.13
40%	0.54	0.76	1.10	1.37
60%	0.31	0.43	0.63	0.76
500 K, 10% C_2H_4				
O_2				
10%	2.42	3.10	5.06	5.89
20%	3.06	3.79	6.04	6.88
40%	3.87	4.80	7.56	8.79
60%	4.59	5.31	8.33	9.84

Table 3
Measured ethylene conversions for silver and Cu–Ag bimetallic catalysts from batch B at 500–540 K and ethylene and oxygen feed concentrations of 10–60%

	Ag	0.2% Cu–Ag	1.0% Cu–Ag
540 K, 10% O_2			
C_2H_4			
10%	1.66	4.72	6.64
20%	0.94	2.69	3.84
40%	0.50	1.39	2.06
60%	0.33	0.88	1.34
540 K, 10% C_2H_4			
O_2			
10%	1.66	4.72	6.64
20%	2.25	5.71	8.18
40%	2.68	7.12	10.20
60%	2.96	8.15	11.59
520 K, 10% O_2			
C_2H_4			
10%	1.02	2.93	4.16
20%	0.57	1.62	2.37
40%	0.29	0.81	1.22
60%	0.18	0.49	0.76
520 K, 10% C_2H_4			
O_2			
10%	1.02	2.93	4.16
20%	1.29	3.49	5.32
40%	1.63	4.32	6.45
60%	1.85	5.03	7.33
500 K, 10% O_2			
C_2H_4			
10%	0.57	1.70	2.64
20%	0.30	0.92	1.46
40%	0.15	0.44	0.72
60%	0.09	0.25	0.42
500 K, 10% C_2H_4			
O_2			
10%	0.57	1.70	2.64
20%	0.74	2.13	3.13
40%	0.93	2.55	3.90
60%	1.06	2.83	4.34

adversely affected by an increase in ethylene feed pressure, with the activation energy increasing from 13.4 to 17.7 kcal/mol. For increasing oxygen feed pressure, the activation energy did not appear to be affected significantly, with measured activation energies ranging from 12.8 to 13.4 kcal/mol. The observed increase in activation energy with increasing ethylene feed pressure can be rationalized as either site blockage by ethylene, which is temperature dependent, or by an increased activation barrier for dissociative oxygen adsorption on more reduced surfaces. In either case, one would expect a shift toward oxygen dissociation becoming rate-determining at lower temperatures and higher ethylene pressure.

Table 4 summarizes the activation energies measured for both silver and Cu–Ag bimetallic catalysts from batches A and B for ethylene consumption and EO and carbon dioxide formation. The silver catalyst from batch B displayed similar activation energy variations with ethylene and oxygen feed pressures to the silver catalyst from batch A. The activation energy increased from 14.3 to 17.9 kcal/mol with increasing ethylene feed pressure while showing no measurable dependence on oxygen feed pressure; the activation energies obtained at different oxygen feed pressures ranged from 13.7 to 14.2 kcal/mol. Activation energies for EO and carbon dioxide formation measured for the silver catalysts from batches A and B ranged from 10.9 to 14.5 kcal/mol and from 14.3 to 20.7 kcal/mol, respectively. These values are in good agreement with the literature values outlined in Table 1.

The activation energies measured for Cu–Ag bimetallic catalysts from batches A and B are also given in Table 4. It is evident that the bimetallic catalysts exhibited similar activation energy trends for ethylene consumption, with the measured values increasing with increasing ethylene feed pressure, while

showing no significant dependence on oxygen feed pressure. In addition, the bimetallic catalysts were characterized by activation energies for ethylene consumption of the order of 1–2 kcal/mol lower than those for the silver catalysts, in good agreement with the enhanced activity of these catalysts displayed in Figs. 3, 5, and 6.

Representative reaction order data for ethylene consumption for a silver catalyst (from batch A) are shown in Figs. 9 and 10. The data are presented as a function of reaction temperature for both ethylene-rich and oxygen-rich conditions. Reaction orders were determined based on the feed pressures of the reactants by assuming power law kinetics as discussed previously. As shown in Fig. 5, the effect of ethylene feed pressure on the reaction rate was not significant. This can be seen in Fig. 9, in which the ethylene reaction orders ranged from 0th order at 540 K to approximately −0.3th order at 500 K for a feed stream consist-

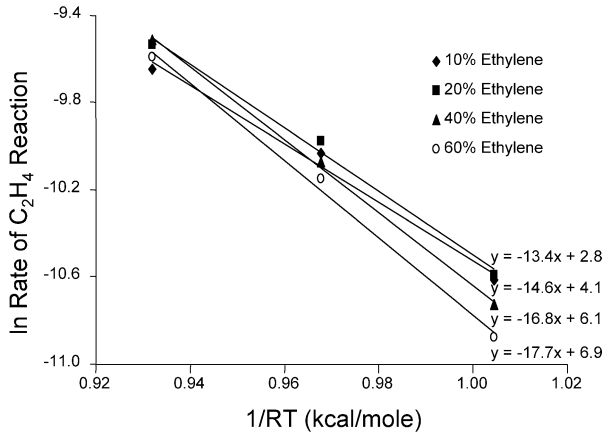

Fig. 7. Activation energy measurements for ethylene consumption over a silver catalyst from batch A as a function of ethylene feed concentration. The reaction rates were measured for a feed stream consisting of 10% oxygen at 500–540 K.

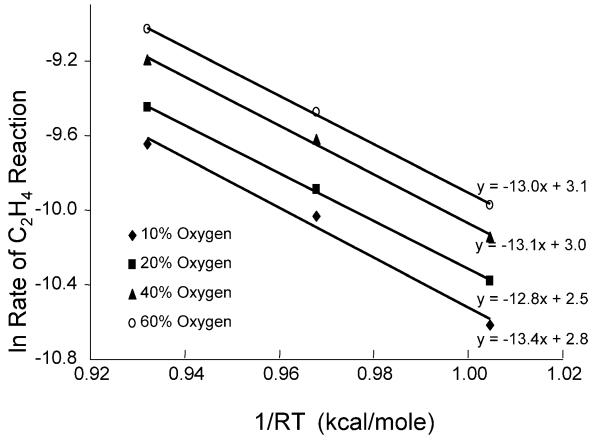

Fig. 8. Activation energy measurements for ethylene consumption over a silver catalyst from batch A as a function of oxygen feed concentration. The reaction rates were measured for a feed stream consisting of 10% ethylene at 500–540 K.

Table 4
Measured activation energies for the consumption of ethylene ($R_{C_2H_4}$) and the formation of ethylene oxide (R_{EO}) and carbon dioxide (R_{CO_2}) for catalysts from batches A and B as a function of feed composition. Activation energies were measured at 500–540 K and are reported in kcal/mol

Batch A												
10% O_2	Ag			0.2% Cu–Ag			0.5% Cu–Ag			1.0% Cu–Ag		
C_2H_4	$R_{C_2H_4}$	R_{EO}	R_{CO_2}	$R_{C_2H_4}$	R_{EO}	R_{CO_2}	$R_{C_2H_4}$	R_{EO}	R_{CO_2}	$R_{C_2H_4}$	R_{EO}	R_{CO_2}
10%	13.0	10.6	13.9	12.3	9.8	13.8	12.4	10.0	13.9	12.0	9.4	13.7
20%	14.2	10.8	15.7	13.0	10.3	14.9	13.4	10.6	15.4	13.0	10.0	15.1
40%	16.3	12.7	18.2	14.6	11.8	17.1	15.6	12.5	18.1	14.6	11.1	17.2
60%	17.2	14.1	19.3	16.4	13.9	18.8	16.4	14.0	18.6	16.1	12.5	19.0
10% C_2H_4	Ag			0.2% Cu–Ag			0.5% Cu–Ag			1.0% Cu–Ag		
O_2	$R_{C_2H_4}$	R_{EO}	R_{CO_2}	$R_{C_2H_4}$	R_{EO}	R_{CO_2}	$R_{C_2H_4}$	R_{EO}	R_{CO_2}	$R_{C_2H_4}$	R_{EO}	R_{CO_2}
10%	13.4	10.9	14.3	12.3	9.8	13.8	12.4	10.0	13.9	12.0	9.4	13.7
20%	12.8	10.9	13.7	12.1	10.0	13.7	12.3	10.6	13.8	11.9	9.9	13.5
40%	13.1	12.3	13.6	12.4	11.2	13.6	12.5	11.2	13.7	12.0	10.4	13.5
60%	13.4	13.0	13.0	13.1	11.9	14.3	12.9	11.8	13.9	11.9	10.3	13.5

Batch B									
10% O_2	Ag			0.2% Cu–Ag			1.0% Cu–Ag		
C_2H_4	$R_{C_2H_4}$	R_{EO}	R_{CO_2}	$R_{C_2H_4}$	R_{EO}	R_{CO_2}	$R_{C_2H_4}$	R_{EO}	R_{CO_2}
10%	14.3	11.6	15.5	13.7	11.5	14.8	12.4	9.8	13.4
20%	15.4	11.8	16.9	14.3	11.4	15.9	12.9	9.9	14.2
40%	16.1	12.0	18.2	15.4	11.1	18.0	14.2	10.2	15.8
60%	17.5	12.4	20.2	16.8	11.9	19.9	15.6	10.8	17.7
10% C_2H_4	Ag			0.2% Cu–Ag			1.0% Cu–Ag		
O_2	$R_{C_2H_4}$	R_{EO}	R_{CO_2}	$R_{C_2H_4}$	R_{EO}	R_{CO_2}	$R_{C_2H_4}$	R_{EO}	R_{CO_2}
10%	14.3	11.6	15.5	13.7	11.4	14.8	12.4	9.8	13.4
20%	14.9	12.2	16.2	13.2	11.2	14.3	12.9	10.4	12.2
40%	14.2	12.4	15.3	13.8	12.0	14.9	12.9	10.7	14.2
60%	13.8	12.2	14.9	14.2	12.4	15.4	13.2	11.1	14.5

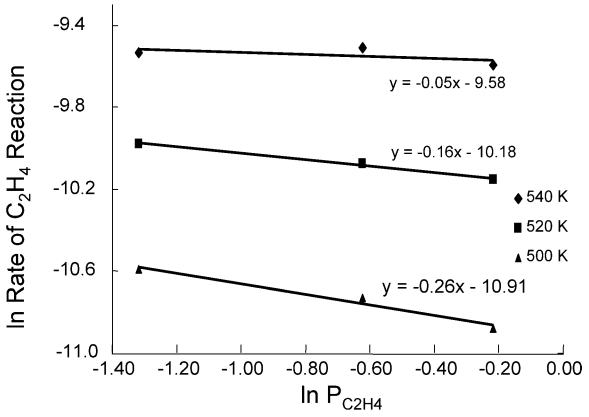

Fig. 9. Measured ethylene reaction orders for ethylene consumption for feed streams containing 10–60% (0.27–0.80 atm) ethylene and 10% (0.13 atm) oxygen as a function of reaction temperature.

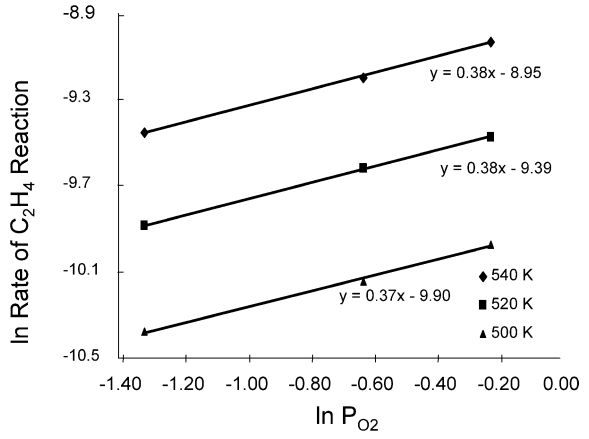

Fig. 10. Measured oxygen reaction orders for ethylene consumption for feed streams containing 10–60% (0.27–0.80 atm) oxygen and 10% (0.13 atm) ethylene as a function of reaction temperature.

ing of 0.13 atm of oxygen and 0.27–0.8 atm of ethylene. Fig. 10 confirms the results of Fig. 6, showing that the rate of consumption increased with increasing oxygen feed pressure. Oxygen reaction orders were approximately 0.4 at all temperatures investigated. Similar trends were observed for a silver catalyst from batch B, for which the ethylene reaction order decreased slightly with decreasing temperature, with values ranging from 0.03 to −0.1, whereas the oxygen reaction order was approximately 0.3 at all temperatures. Tables 5 and 6 summarize the measured reaction orders for the consumption of ethylene over silver and Cu–Ag bimetallic catalysts from batches A and B. Although the ethylene reaction orders varied slightly for the catalysts investigated, there was a consistent transition from the 0th to negative order as the catalyst temperature was decreased from 540 to 500 K. The oxygen reaction orders were measured in the range of 0.3–0.4 for all samples investigated, with little or no dependence on reaction temperature.

The presence of 0th to negative ethylene reaction orders indicates that for ethylene-rich feed conditions, the rate-determining step of the reaction is dissociative adsorption of oxygen. Positive oxygen reaction orders indicate that under oxygen-rich conditions, the rate-determining step of the reaction could be either dissociative adsorption of oxygen or the surface reaction of adsorbed ethylene with adsorbed oxygen. To determine which of these two steps was rate-determining, the ethylene reaction order was measured for oxygen-rich streams containing 10–30% (0.13–0.34 atm) ethylene and 60% (0.8 atm) oxygen. These values are listed in Table 7 for a silver catalyst and a 0.2% Cu–Ag bimetallic catalyst from batch A. As can be seen, the ethylene reaction orders varied from 0.3 to 0.5 for temperatures of 500–540 K. The positive ethylene reaction orders indicate that the rate-determining step under oxygen-rich conditions is the surface reaction step. Therefore, the rate-determining step of the reaction is governed by the

Table 5
Ethylene and oxygen reaction orders measured for silver and Cu–Ag bimetallic catalysts from batch A for the consumption of ethylene ($R_{C_2H_4}$) and the formation of ethylene oxide (R_{EO}) and carbon dioxide (R_{CO_2}) as a function of ethylene pressure (P_{C_2}) and oxygen pressure (P_{O_2}) for reaction temperatures of 500–540 K assuming power law kinetics

	500 K		520 K		540 K	
	P_{C_2}	P_{O_2}	P_{C_2}	P_{O_2}	P_{C_2}	P_{O_2}
Ag						
$R_{C_2H_4}$	−0.26	0.37	−0.16	0.38	−0.05	0.38
R_{EO}	−0.03	0.52	0.09	0.58	0.19	0.65
R_{CO_2}	−0.4	0.27	−0.29	0.26	−0.15	0.23
0.2% Cu–Ag						
$R_{C_2H_4}$	−0.23	0.31	−0.16	0.33	0	0.37
R_{EO}	−0.09	0.44	0.1	0.51	0.14	0.57
R_{CO_2}	−0.36	0.19	−0.31	0.16	−0.09	0.22
0.5% Cu–Ag						
$R_{C_2H_4}$	−0.31	0.3	−0.2	0.31	−0.1	0.33
R_{EO}	−0.2	0.4	−0.05	0.45	0.2	0.48
R_{CO_2}	−0.41	0.2	−0.32	0.18	−0.18	0.21
1% Cu–Ag						
$R_{C_2H_4}$	−0.28	0.33	−0.14	0.3	−0.08	0.33
R_{EO}	−0.14	0.44	−0.02	0.43	0.02	0.47
R_{CO_2}	−0.4	0.21	−0.24	0.17	−0.13	0.22

Table 6
Ethylene and oxygen reaction orders measured for silver and Cu–Ag bimetallic catalysts from batch B for the consumption of ethylene ($R_{C_2H_4}$) and the formation of ethylene oxide (R_{EO}) and carbon dioxide (R_{CO_2}) as a function of ethylene pressure (P_{C_2}) and oxygen pressure (P_{O_2}) for reaction temperatures of 500–540 K assuming power law kinetics

	500 K		520 K		540 K	
	P_{C_2}	P_{O_2}	P_{C_2}	P_{O_2}	P_{C_2}	P_{O_2}
Ag						
$R_{C_2H_4}$	−0.09	0.33	−0.04	0.33	0.03	0.29
R_{EO}	0.08	0.47	0.08	0.5	0.09	0.51
R_{CO_2}	−0.18	0.24	−0.1	0.23	0.01	0.18
0.2% Cu–Ag						
$R_{C_2H_4}$	−0.17	0.26	−0.08	0.33	−0.01	0.32
R_{EO}	0.01	0.42	0.02	0.46	0.04	0.5
R_{CO_2}	−0.3	0.15	−0.13	0.25	−0.03	0.23
1% Cu–Ag						
$R_{C_2H_4}$	−0.13	0.3	−0.03	0.29	0.05	0.32
R_{EO}	−0.01	0.41	0.05	0.45	0.05	0.46
R_{CO_2}	−0.19	0.23	−0.06	0.2	0.05	0.24

Table 7
Ethylene reaction orders measured for silver and Cu–Ag bimetallic catalysts from batch A for the consumption of ethylene ($R_{C_2H_4}$) and the formation of ethylene oxide (R_{EO}) and carbon dioxide (R_{CO_2}) for ethylene pressures ($P_{C_2H_4}$) of 0.27–0.8 atm and 0.13–0.4 atm and oxygen pressures of 0.13 and 0.8 atm, respectively, as a function of reaction temperature assuming power law kinetics

	500 K	520 K	540 K
$P_{O_2} = 0.13$ atm, $P_{C_2H_4} = 0.27$–0.8 atm			
Ag			
$R_{C_2H_4}$	−0.26	−0.16	−0.05
R_{EO}	−0.03	0.09	0.19
R_{CO_2}	−0.4	−0.29	−0.15
0.2% Cu–Ag			
$R_{C_2H_4}$	−0.23	−0.16	0
R_{EO}	−0.09	0	0.05
R_{CO_2}	−0.33	−0.26	−0.02
$P_{O_2} = 0.8$ atm, $P_{C_2H_4} = 0.13$–0.4 atm			
Ag			
$R_{C_2H_4}$	0.26	0.28	0.38
R_{EO}	0.31	0.31	0.39
R_{CO_2}	0.21	0.25	0.37
0.2% Cu–Ag			
$R_{C_2H_4}$	0.26	0.38	0.48
R_{EO}	0.22	0.36	0.48
R_{CO_2}	0.3	0.39	0.46

feed compositions and temperatures used, with more ethylene-rich conditions being rate-controlled by oxygen adsorption and more oxygen-rich conditions being rate-controlled by the surface reaction of adsorbed ethylene and oxygen.

Tables 5 and 6 also give the measured ethylene reaction orders for EO and carbon dioxide formation for silver and Cu–Ag bimetallic catalysts from batches A and B. Ethylene reaction orders for EO formation varied from 0.2 to −0.2 for catalysts from batch A, with the reaction orders decreasing with decreasing reaction temperature. A similar trend was observed for carbon dioxide formation, with values varying from −0.2 to −0.4. Catalysts from batch B showed almost no temperature dependence of the ethylene reaction order with respect to EO formation. The measured ethylene reaction orders appeared to be approximately 0th order for all catalysts examined. A different trend was observed for carbon dioxide formation, with ethylene reaction orders varying from 0th order to −0.3th order for the catalysts examined. As observed for catalysts from batch A, the ethylene reaction order decreased with decreasing reaction temperature.

Also reported in Tables 5 and 6 are the oxygen reaction orders for EO and carbon dioxide formation. Catalysts from batch A showed oxygen reaction orders for EO formation ranging from 0.4 to 0.7, with only minor variations with reaction temperature observed. Oxygen reaction orders for carbon dioxide formation ranged from 0.2 to 0.3 for all catalysts examined. As was observed for ethylene reaction, carbon dioxide formation exhibited no measurable temperature dependence with respect to the oxygen reaction order. Catalysts from batch B had an oxygen reaction order of approximately 0.5 for EO formation for all catalysts examined, whereas reaction orders for carbon dioxide formation were approximately 0.2.

The measured ethylene and oxygen reaction orders provide a means to examine how the reactants influence the formation of products and, in general, provide an indirect way to determine changes in product distribution with changing feed composition. From the ethylene reaction order data, it appears that for ethylene-rich conditions, increasing the ethylene feed pressure lowers the activity of the catalyst. In addition, it is evident that carbon dioxide formation is characterized by a more negative dependence on ethylene feed pressure than EO formation for all catalysts and conditions examined. This finding demonstrates that ethylene can serve to promote the selectivity of the catalyst at the expense of some activity. Previous work by Monnier et al. [24] has shown a similar beneficial effect on selectivity from increasing olefin concentration in butadiene epoxidation. In contrast to the effect of ethylene in our experiments, oxygen significantly increased the activity of the catalyst. In addition, the measured oxygen reaction orders for individual products indicate that EO formation has a more positive dependence on oxygen than does carbon dioxide formation. Therefore, oxygen promotes both the activity and selectivity of the catalyst by increasing the formation of EO relative to that of carbon dioxide. This result is somewhat counterintuitive, based on the concept that more oxygen-rich conditions should drive up the rate of formation of combustion products relative to selective oxidation products. However, although it is clear that combustion rates do increase with increasing oxygen feed pressure, as evidenced by the positive reaction order measurements for carbon dioxide formation, these rates do not increase to the same extent as those for epoxide formation. The observed trends for increasing ethylene and oxygen feed pressures suggest that the selectivity to EO should increase with increasing total reactant pressures.

Feed variations were also studied to examine the efficacy of the Cu–Ag bimetallic catalysts relative to pure silver with respect to EO selectivity at similar ethylene conversions. The major purpose was to determine whether the selectivity enhancements of the bimetallic catalysts were sustained for both ethylene-rich and oxygen-rich feed stoichiometries, as well as for equimolar feeds at higher pressure. These data are presented in Figs. 11 and 12 for catalysts from batch A. The corresponding ethylene conversion data are given in Table 8. Fig. 11 shows selectivity data for silver and Cu–Ag bimetallic catalysts from batch A for feed streams containing ethylene-to-oxygen ratios ranging from 1:1 to 6:1 at similar ethylene conversions. Feed variations were conducted by maintaining the oxygen feed concentration at 10% (0.13 atm) and increasing the ethylene feed concentration from 10 to 60% (0.13–0.8 atm). The data for each catalyst shown in Fig. 11 were collected at constant temperature, with the temperature of each catalyst sample adjusted to give an ethylene conversion of approximately 1.8% for a 1:1 feed stoichiometry (0.13 atm each of ethylene and oxygen). This temperature was then maintained as the ethylene pressure was increased. The similar kinetic dependences observed for both the silver and Cu–Ag bimetallic catalysts with respect to ethylene pressure led to comparable ethylene conversions for

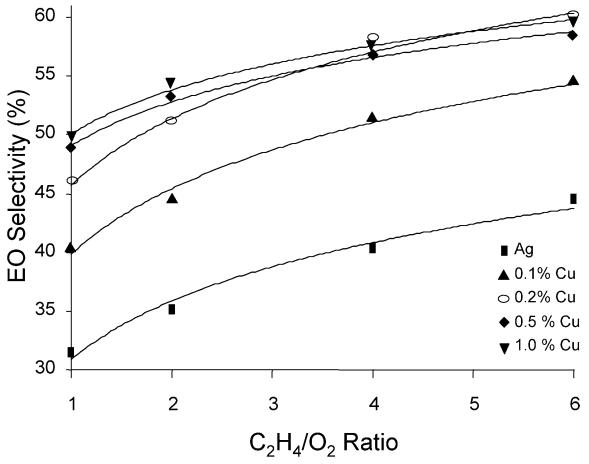

Fig. 11. EO selectivity for silver and Cu–Ag bimetallic catalysts from batch A as a function of feed stoichiometry for ethylene-rich feed conditions.

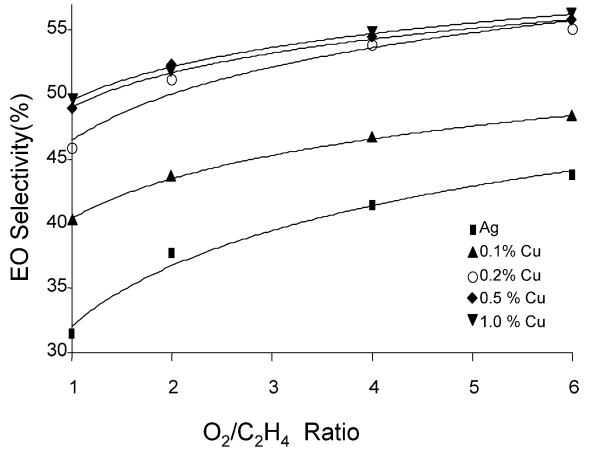

Fig. 12. EO selectivity for silver and Cu–Ag bimetallic catalysts from batch A as a function of feed stoichiometry for oxygen-rich feed conditions.

Table 8
Ethylene conversion data obtained for silver and Cu–Ag bimetallic catalysts from batch A for ethylene and oxygen feed pressures of 0.13–0.8 atm collected at constant temperature. The temperatures used to conduct the measurements were selected to give a conversion of approximately 1.8% for a feed stream consisting of 0.13 atm each of ethylene and oxygen. These temperatures are listed in parentheses next to each catalyst

$P_{C_2H_4}$	P_{O_2}	Ag (490 K)	0.1% Cu–Ag (475 K)	0.2% Cu–Ag (481 K)	0.5% Cu–Ag (470 K)	1.0% Cu–Ag (459 K)
0.13	0.13	1.81	1.82	1.80	1.81	1.83
0.27	0.13	0.90	0.76	0.78	0.72	0.71
0.54	0.13	0.38	0.33	0.30	0.30	0.28
0.8	0.13	0.22	0.19	0.18	0.17	0.17
0.13	0.27	2.18	2.57	2.46	2.47	2.54
0.13	0.54	2.97	3.40	3.26	3.40	3.54
0.13	0.8	3.58	3.79	3.72	3.80	3.87
0.27	0.27	1.30	1.25	1.21	1.15	1.14
0.54	0.27	0.55	0.51	0.51	0.47	0.46
0.27	0.54	1.62	1.73	1.65	1.70	1.71
0.54	0.54	0.88	0.84	0.85	0.79	0.78

each set of feed conditions. The observed conversions varied from approximately 1.8% at a 1:1 stoichiometry to approximately 0.2% at a 6:1 stoichiometry. As shown in Fig. 11, the selectivity to EO increased with increasing ethylene pressure. The maximum selectivity to EO observed for the supported silver catalyst was approximately 45% and occurred with an ethylene-to-oxygen feed ratio of 6:1. The Cu–Ag bimetallic catalysts were shown to perform extremely well relative to pure silver for ethylene-rich conditions, a result that was consistent for both batches A and B. Maximum EO selectivities of 58–59% were observed for the 0.2–1.0% Cu–Ag bimetallic catalysts from batch A at a feed composition of 6:1 ethylene to oxygen.

Similar studies were conducted for oxygen-rich feed conditions. Feed variations were conducted by maintaining the ethylene feed concentration at 10% and increasing the oxygen feed concentration from 10 to 60%. The similar kinetic dependencies observed for both the silver and Cu–Ag bimetallic catalysts with respect to oxygen pressure led to comparable ethylene conversions for each set of feed conditions. For these studies, the ethylene conversion varied from approximately 1.8% for an oxygen-to-ethylene ratio of 1:1 to approximately 3.5% for a ratio of 6:1. These data are shown in Fig. 12 for catalysts from batch A. The selectivity to EO increased with increasing oxygen feed pressure, with a maximum observed EO selectivity of 44% for a silver catalyst from batch A at a feed composition of 6:1 oxygen to ethylene. It is evident that the Cu–Ag bimetallic catalysts outperformed the pure silver catalysts even under the most oxygen-rich conditions, in which the propensity for combustion should be enhanced. The ability of copper to act as a total oxidation catalyst may lead to the potential for diminished performance of the bimetallic catalysts under severe oxidizing conditions. However, there did not appear to be any significant loss of performance relative to pure silver for the conditions studied. Maximum selectivities to EO of 55–56% were observed for the 0.2–1.0% Cu–Ag bimetallic catalysts from batch A at a feed composition of 6:1 oxygen to ethylene.

The performance of silver and Cu–Ag bimetallic catalysts was also examined by simultaneously varying both the ethylene and oxygen feed pressures in a range of 0.13–0.54 atm. From these data, three-dimensional selectivity contours were generated at constant temperature to examine the effects of feed pressure and stoichiometry on EO selectivity. These results are shown in Fig. 13 for both silver and 0.2% Cu–Ag bimetallic catalysts at similar ethylene conversions. It appears that selectivity to EO increased in the direction of increasing ethylene and oxygen pressure, with the highest measured selectivity observed for a feed consisting of 0.54 atm of ethylene and oxygen. In addition, it is apparent that the bimetallic catalysts outperformed pure silver over the entire range of feed compositions investigated, with maximum observed selectivity to EO of 49% for the silver catalyst and 60% for the 0.2% Cu–Ag bimetallic catalyst from batch A. Additional measurements were conducted for 0.1, 0.5, and 1.0% Cu–Ag bimetallic catalysts from batch A as well as for a 1.0% Cu–Ag catalyst from batch B. The selectivity data for these catalysts and for the silver and 0.2% Cu–Ag catalysts are summarized in Table 9, along with the temperatures used to conduct the measurements. As expected, the bimetallic catalysts afforded lower operating temperatures than silver, by as much as 30 and 55 K for 1.0%

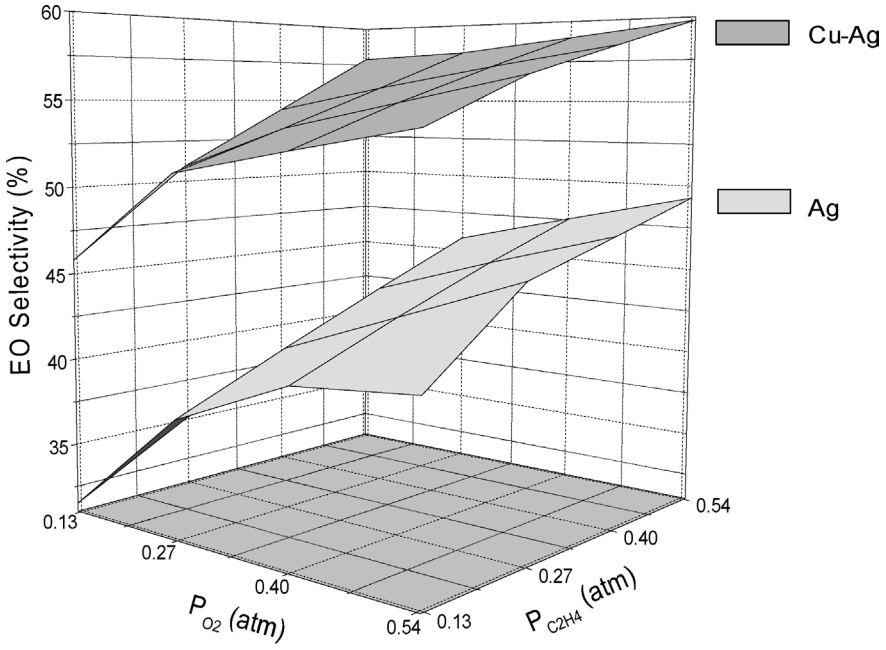

Fig. 13. 3D contours of EO selectivity for a silver and a 0.2% Cu–Ag bimetallic catalyst from batch A for ethylene and oxygen pressures ranging 0.13–0.54 atm.

Table 9
EO selectivity data obtained for silver and Cu–Ag bimetallic catalysts from batches A and B for ethylene and oxygen feed pressures of 0.13–0.54 atm collected at constant temperature. The temperatures used to conduct the measurements were selected to give a conversion of approximately 1.6–1.8% for a feed stream consisting of 0.13 atm each of ethylene and oxygen. These temperatures are listed in parentheses next to each catalyst

Batch A

$P_{C_2H_4}$	P_{O_2}	Ag (490 K)	0.1% Cu–Ag (475 K)	0.2% Cu–Ag (480 K)	0.5% Cu–Ag (470 K)	1.0% Cu–Ag (459 K)
0.13	0.13	31.5	40.3	45.8	48.8	49.7
0.27	0.13	35.1	44.5	50.9	53.1	54.4
0.54	0.13	40.3	51.4	57.9	56.8	57.7
0.13	0.27	37.7	43.7	51.1	52.2	52.1
0.13	0.54	40.7	46.6	53.8	54.4	54.6
0.27	0.27	40.5	46.7	53.4	55.0	55.9
0.54	0.27	45.8	51.8	58.2	58.3	59.5
0.27	0.54	45.9	49.0	56.4	56.1	57.4
0.54	0.54	49.3	52.5	59.8	59.1	60.4

Batch B

$P_{C_2H_4}$	P_{O_2}	Ag (490 K)	0.2% Cu–Ag (480 K)	1.0% Cu–Ag (459 K)
0.13	0.13	25.9	35.2	34.9
0.27	0.13	26.4	37.8	37.6
0.54	0.13	27.5	43	42.0
0.13	0.27	29.7	37.1	37.5
0.13	0.54	35.2	41.8	40.9
0.27	0.27	32.7	41.4	39.6
0.54	0.27	34.5	44.7	42.8
0.27	0.54	35.5	44.1	42.5
0.54	0.54	36.6	45.8	44.3

Cu–Ag catalysts from batches A and B, to achieve comparable ethylene conversions. The data in Table 9 also indicate that all of the bimetallic catalysts examined were more selective to EO compared with silver for the entire range of conditions examined.

4. Discussion

The results of kinetic studies conducted on silver and Cu–Ag bimetallic catalysts showed that the performance of these catalysts, in terms of both activity and selectivity as well as the identity of the rate-determining step, was dependent on the reactant feed stoichiometry. For ethylene-rich feeds, the rate of reaction was controlled by the dissociative adsorption of oxygen. As the ethylene pressure was increased (at constant oxygen pressure), the rate of reaction remained constant or decreased slightly, while the selectivity to EO increased slightly. The increase in EO selectivity resulted from a larger decrease in the formation rate of carbon dioxide relative to EO. In addition, the measured activation energy for ethylene consumption increased as the ethylene pressure increased. This activity and selectivity behavior can be explained by the action of ethylene as a site blocker, especially if ethylene also blocks sites that may be active for ethylene or EO combustion or isomerization. This explanation is supported by the temperature dependence observed for the ethylene reaction orders, which become more negative with decreasing reaction temperature. The observed increase in apparent activation energy can be explained by a larger ethylene surface coverage at lower temperatures, the effect of which becomes more significant at higher ethylene pressures.

A different trend was observed when the ethylene pressure was increased under oxygen-rich conditions, in which case an increase in ethylene feed pressure was accompanied by an increase in reaction rate. This behavior indicates that under oxygen-rich conditions, the reaction rate is controlled by the surface reaction of adsorbed ethylene and oxygen. Although the exact stoichiometric point of transition (between adsorption-controlled and surface reaction-controlled) in the rate-determining step is not known, the data presented in Fig. 5

Table 10
Ethylene reaction orders measured for silver and Cu–Ag bimetallic catalysts from batch A for the consumption of ethylene at an oxygen pressure of 0.13 atm and ethylene pressures of 0.13–0.27 atm, 0.27–0.54 atm, and 0.54–0.8 atm, respectively, as a function of reaction temperature assuming power law kinetics

$P_{O_2} = 0.13$ atm $P_{C_2H_4}$ (atm)	500 K	520 K	540 K
	Ag		
0.13–0.27	0.04	0.08	0.16
0.27–0.54	−0.2	−0.14	0.03
0.54–0.8	−0.37	−0.2	−0.2
	0.2% Cu–Ag		
0.13–0.27	0.1	0.18	0.18
0.27–0.54	−0.12	0.01	0.05
0.54–0.8	−0.44	−0.12	−0.1
	0.5% Cu–Ag		
0.13–0.27	0.07	0.18	0.18
0.27–0.54	−0.27	−0.12	−0.04
0.54–0.8	−0.39	−0.36	−0.23
	1.0% Cu–Ag		
0.13–0.27	0.09	0.21	0.19
0.27–0.54	−0.19	−0.1	−0.03
0.54–0.8	−0.45	−0.22	−0.18

indicate that at 540 K, the transition occurs at an ethylene-to-oxygen ratio of approximately 2:1. Fig. 5 shows an increase in the measured rate of reaction from a 1:1 to a 2:1 ethylene-to-oxygen stoichiometry, followed by leveling or a decreasing rate for higher stoichiometric ratios. To further study this transition in the rate-determining step, the ethylene reaction orders were measured for silver and Cu–Ag bimetallic catalysts from batch A for an oxygen pressure of 0.13 atm and ethylene pressure ranges of 0.13–0.27 atm, 0.27–0.54 atm, and 0.54–0.8 atm; the results are given in Table 10. The measured reaction orders decreased from approximately 0.2 in an ethylene pressure range of 0.13–0.27 atm to approximately −0.2 for an ethylene pressure range of 0.54–0.8 atm at 540 K. This indicates that the rate-determining step of the reaction transitions from surface reaction-controlled to adsorption-controlled with this increase in ethylene pressure. A similar decrease was observed for the reaction orders at 500 and 520 K. This observed transition in rate control between oxygen adsorption and surface reaction has been presented in a microkinetic model developed by Stegelmann et al. [9]. These authors showed that the effect of ethylene on the catalyst activity is dependent on the reactant stoichiometry. The model showed a transition from a slight positive dependence to slight negative dependence of the activity at an oxygen pressure of 0.13 atm and increasing ethylene pressures of 0.27–0.8 atm and showed a positive dependence at an oxygen pressure of 0.8 atm and increasing ethylene pressures of 0.13–0.40 atm, both of which are in excellent agreement with observations presented here.

The effect of oxygen feed pressure on reaction rate and selectivity was different than that for ethylene. Unlike ethylene, oxygen was shown to enhance both the activity and selectivity of the process with increasing feed pressure. This dramatic increase in the rate of epoxidation relative to the rate of combustion can be attributed to an increase in the concentration of subsurface oxygen. The role of subsurface oxygen has been studied extensively. Recent DFT studies by Mavrikakis et al. [25] indicate that subsurface oxygen decreases the barrier to and increases the rate constant for dissociative adsorption of oxygen on Ag(111). It has also been suggested that the subsurface oxygen modifies the electronic properties of the surface oxygen atoms in its vicinity, so that they become more vulnerable to attack by the C=C bond in ethylene [26,27]. It has even been proposed that subsurface oxygen is the catalytically active phase [28]. Our design of Cu–Ag bimetallic catalysts is predicated on the involvement of the oxametallacycle intermediate in both the selective and nonselective reaction pathways [7]. The nonselective pathway involves the formation of acetaldehyde, which then quickly combusts to form carbon dioxide. The formation of acetaldehyde occurs via an H-atom shift from the central carbon to the terminal carbon of the oxametallacycle. In general, any selectivity enhancement would involve a decreased rate of H-atom shift, and hence acetaldehyde formation, relative to epoxide formation. Therefore, one possible role of subsurface oxygen is to inhibit the H-atom shift of the oxametallacycle. This is consistent with the roles of adsorbed cations and subsurface anions in influencing the competing transition states for oxametallacycle reactions through alteration of the surface electric field suggested previously [29].

In addition to being more selective for ethylene epoxidation, the Cu–Ag bimetallic catalysts were more active than pure silver for all copper loadings investigated. This increased activity was illustrated by the activation energy measurements, in which the bimetallic samples had activation energies for ethylene consumption on the order of 1–2 kcal/mol lower than those for pure silver. This is an uncommon phenomenon for ethylene epoxidation, because the typical promoters (e.g., cesium and chlorine) tend to increase EO selectivity at the expense of activity [6]. The increase in activity can most likely be attributed to an increase in the rate of oxygen dissociation on the catalyst surface.

An interesting result of the kinetic studies is the similarities of the silver and Cu–Ag bimetallic catalysts. In addition to having similar activation energies for ethylene consumption and product formation, the silver and Cu–Ag bimetallic catalysts showed very similar trends with respect to the ethylene and oxygen reaction orders, for both ethylene consumption and product formation. This indicates that modifying the silver surface with small amounts of copper does not significantly affect the mechanism or underlying kinetics of the process, and therefore justifies the assumptions behind our computational model [7]. As noted above, copper's major effect on reaction kinetics is to lower the activation barrier for oxygen adsorption. The kinetic studies also showed that, independent of which of the steps leading to oxametallacycle formation is rate-determining under a given set of conditions, the Cu–Ag bimetallic catalysts are more effective for ethylene epoxidation than pure silver catalysts under all conditions.

5. Conclusion

A series of silver and Cu–Ag bimetallic catalysts were studied over a wide range of temperatures and reactant feed pressures. Analysis of the kinetics showed that the rate-determining step of the reaction was dependent on the feed compositions used. Similar kinetic dependences were observed for both the silver and bimetallic samples. Activation energy measurements showed a 1–2 kcal/mol decrease in ethylene consumption for the Cu–Ag bimetallic catalysts relative to pure silver. In addition, the Cu–Ag bimetallic catalysts were shown to be more selective for EO formation over a wide range of reactant feed stoichiometries than pure silver catalysts at similar ethylene conversions.

Acknowledgments

We gratefully acknowledge the support of the U.S. Department of Energy, Division of Chemical Sciences (grant FG02-84ER13290).

References

[1] D. Denton, S. Falling, J. Monnier, J. Stavinoha, W. Watkins, Chim. Oggi—Chem. Today 14 (1996) 17.
[2] R.K. Grasselli, J.D. Burrington, Adv. Catal. 30 (1981) 133.
[3] Chem. Eng. News 77 (2001) 19.
[4] S. Linic, M.A. Barteau, J. Am. Chem. Soc. 125 (2003) 4034.
[5] E.M. Cordi, J.L. Falconer, Appl. Catal. A: Gen. 151 (1997) 179.
[6] R.A. van Santen, H. Kuipers, Adv. Catal. 35 (1987) 265.
[7] S. Linic, J.T. Jankowiak, M.A. Barteau, J. Catal. 224 (2004) 489.
[8] S. Linic, M.A. Barteau, J. Catal. 214 (2003) 200.
[9] C. Stegelmann, N.C. Schiødt, C.T. Campbell, P. Stoltze, J. Catal. 221 (2004) 630.
[10] C. Stegelmann, P. Stoltze, J. Catal. 226 (2004) 129.
[11] G.H. Twigg, Trans. Faraday Soc. 42 (1946) 284.
[12] K. Murray, Aust. J. Sci. Res. A 3 (1950) 433.
[13] W. Shen-Wu, I&EC Res. 45 (1953) 234.
[14] A.I. Kurilenko, N.V. Kul'kowa, N.A. Rybakowa, M.I. Temkin, Zh. Fiz. Khim. 32 (1958) 797.
[15] F. Fognani, R. Montarnal, Rev. Inst. Fr. Pet. 14 (1959) 191.
[16] F. Alfani, J.J. Carberry, Chim. Ind. (Milan) 52 (1970) 1192.
[17] R.E. Kenson, M. Lapkin, J. Phys. Chem. 74 (1970) 1493.
[18] P.D. Klugherz, P. Harriot, AIChE J. 17 (1971) 856.
[19] P.L. Metcalf, P. Harriott, Ind. Eng. Chem., Prod. Res. Dev. 11 (1972) 478.
[20] A. Verma, S. Kaliaguine, J. Catal. 30 (1973) 430.
[21] E.L. Force, A.T. Bell, J. Catal. 40 (1975) 356.
[22] R.H. Dettwiler, A. Baker, W. Richarz, Helv. Chim. Acta 62 (1979) 1680.
[23] P. Kripylo, L. Mogling, H. Ehrchen, I. Harkanyi, D. Klose, L. Beck, Chem. Tech. (Leipzig) 31 (1979) 82.
[24] J.R. Monnier, K.T. Peters, G.W. Hartley, J. Catal. 225 (2004) 374.
[25] Y. Xu, J. Greeley, M. Mavrikakis, J. Am. Chem. Soc. 127 (2005) 12823.
[26] P.J. van den Hoek, E.J. Baerends, R.A. van Santen, J. Phys. Chem. 93 (1989) 6469.
[27] J.A. Moulijn, V. Ponec, Catalysis: An Integrated Approach to Homogeneous, Heterogeneous and Industrial Catalysis, Elsevier, Amsterdam, 1993.
[28] W.-X. Li, C. Stampfl, M. Scheffler, Phys. Rev. Lett. 90 (2003), Art. No. 256102.
[29] S. Linic, M.A. Barteau, J. Am. Chem. Soc. 126 (2004) 8086.